Therapy-induced senescence mitochondrial proteome reveals a role for ABAT in catabolic reprogramming

Jennyfer Martínez[1], Doménica Tarallo[1], Alejandro Leyva[2], Rodrigo Martino-Kunsch[3], Inés Marmisolle[1], Rafael Sebastián Fort[4], Marcos Tassano[5], Carolina Perroni[5], Guillermo Grünwaldt[1], Gabriel Anderson[6], Andrés López-Radcenco[6], Guillermo Moyna[6], Ernesto Miquel[7], Juan Pablo Gambini[8], Paula Céspedes[9,10], Mariela Bollati-Fogolín[9], Natalia de Isla[11], María Ana Duhagon[12], Mercedes Rodríguez-Teja[3], María Moreno[13], Rosario Durán[2] and Celia Quijano[1].

[1] Departamento de Bioquímica, Facultad de Medicina, and Centro de Investigaciones Biomédicas (CEINBIO), Universidad de la República, Uruguay
[2] Unidad mixta de Bioquímica y Proteómica Analíticas. Institut Pasteur de Montevideo and Instituto de Investigaciones Biológicas Clemente Estable (IIBCE), Uruguay
[3] Departamento de Genética, Facultad de Medicina, Universidad de la República, Uruguay
[4] Sección Genómica Funcional, Facultad de Ciencias, Universidad de la República, Uruguay
[5] Departamento de Radiofarmacia, Centro de Investigaciones Nucleares, Facultad de Ciencias, Universidad de la República, Uruguay
[6] Laboratorio de Química Orgánica, Departamento de Química del Litoral, CENUR Litoral Norte, Universidad de la República, Uruguay
[7] Departamento de Histología y Embriología, Facultad de Medicina, Universidad de la República, Uruguay
[8] Centro Uruguayo de Imagenología Molecular and Centro de Medicina Nuclear, Hospital de Clínicas, Facultad de Medicina, Universidad de la República, Uruguay
[9] Unidad de Biología Celular, Institut Pasteur de Montevideo, Uruguay
[10] Present Address: Advanced Bioimaging Unit, Institut Pasteur de Montevideo and Universidad de la República, Uruguay.
[11] Lorraine University, CNRS UMR 7365, IMoPA laboratory, 54500 Vandoeuvre-lès-Nancy, France.
[12] Sección Genómica Funcional, Facultad de Ciencias and Departamento de Genética, Facultad de Medicina, Universidad de la República, Uruguay
[13] Laboratorio de Vacunas Recombinantes, Unidad Académica de Desarrollo Biotecnológico, Facultad de Medicina, Universidad de la República, Uruguay

* Correspondence should be addressed to: Celia Quijano, email: celiq@fmed.edu.uy; celia.quijano@gmail.com

Supplementary Figures

Figure S1

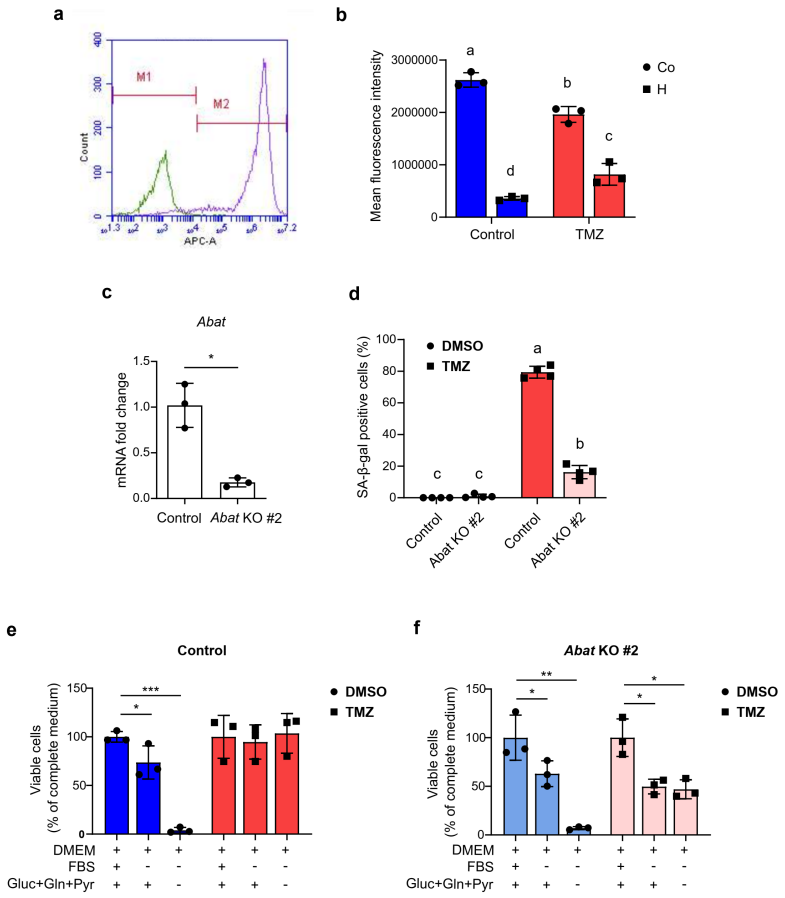


Figure S1. (**a**-**b**) B16-F1 cells were exposed to TMZ (200 µM) to induce senescence or to DMSO (Control) (two 5-hour incubations separated by 24 hours) and evaluated four days after the second exposure. We used the SCENITH method to measure protein synthesis by flow cytometry. **a** Representative histogram of cells with (purple) and without (green) staining with an anti-puromycin antibody. **b** Cells were treated with the protein synthesis inhibitor Harringtonine (H, 2 µg/mL), as a negative control, and puromycin was added (10 µg/ml) at the end of the incubation with H. Mean fluorescence intensity with (H) and without harringtonine (Co) of control and senescent cells is shown (n = 3). (**c-f**) *Abat* expression was knocked out with the CRISPR/Cas9 system; an empty CRISPR-V2 vector was used as a Control. **c** RT-qPCR for *Abat* expression. Results are expressed relative to the Control condition (n = 3). **d** SA-β-gal positive cells after treatment with TMZ (n = 4). **e** and **f** After 24 hours of incubation in the different media, viable cells were counted by trypan blue exclusion and expressed as a percentage relative to cells cultured in complete medium (DMEM supplemented with glucose, glutamine, pyruvate and FBS) in each condition, which was considered 100%. Results are the mean ± S.D. In **c** statistical differences were determined by t-test, * $P < 0.05$. In **b** and **d** statistical differences were determined by two-way ANOVA and Tukey post hoc for multiple comparisons. Groups with different letters are significantly different ($P < 0.05$). In **e** and **f**, statistical differences were determined by one-way ANOVA and Dunnett's post hoc for multiple comparisons; * $P < 0.05$, ** $P < 0.001$, *** $P < 0.0001$.

Figure S2

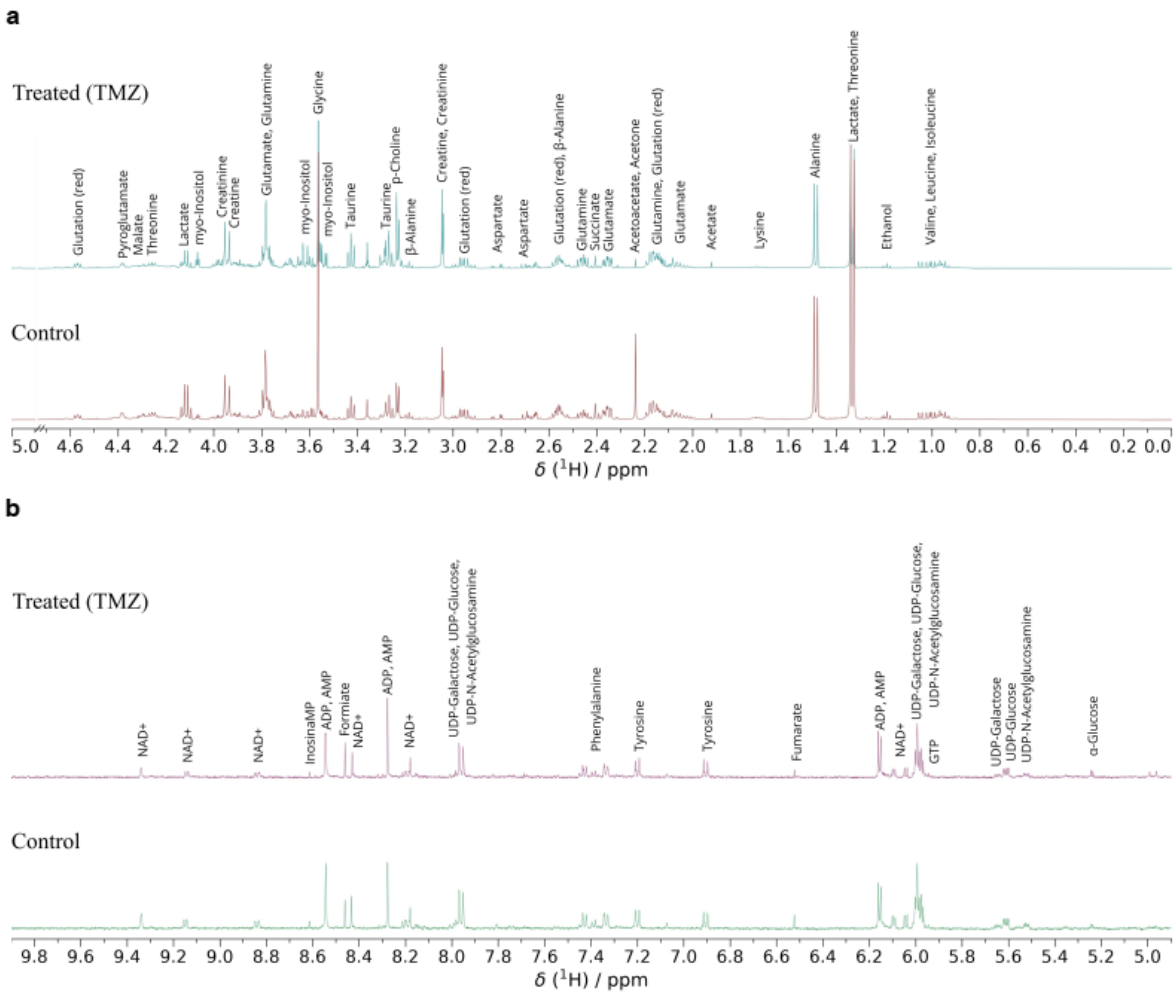


Figure S2. Representative ^{1}H NMR spectra of control and TMZ-treated B16-F1 cells. Representative spectra of intracellular metabolite extracts from DMSO-treated (Control) and TMZ-induced senescent B16-F1 cells. Assigned metabolite peaks are indicated. Chemical shifts are expressed in parts per million (ppm). **a** 0–5 ppm region. **b** 5–10 ppm region

Supplementary Table 1. Mitochondrial respiratory indexes. Coupling efficiency, spare respiratory capacity, and respiratory control ratio calculated from OCR measurements in Fig. 5d. Results are the mean ± S.D. Statistical differences were determined with t-tests, *** $P < 0.0001$.

Respiratory ratios	Control	^{223}Ra
Coupling efficiency	0.56 ± 0.02	0.76 ± 0.02 ***
Spare respiratory capacity	1.96 ± 0.05	2.17 ± 0.35 ^{ns}
Respiratory control ratio	4.5 ± 0.16	9.1 ± 1.7 ***

Figure S3

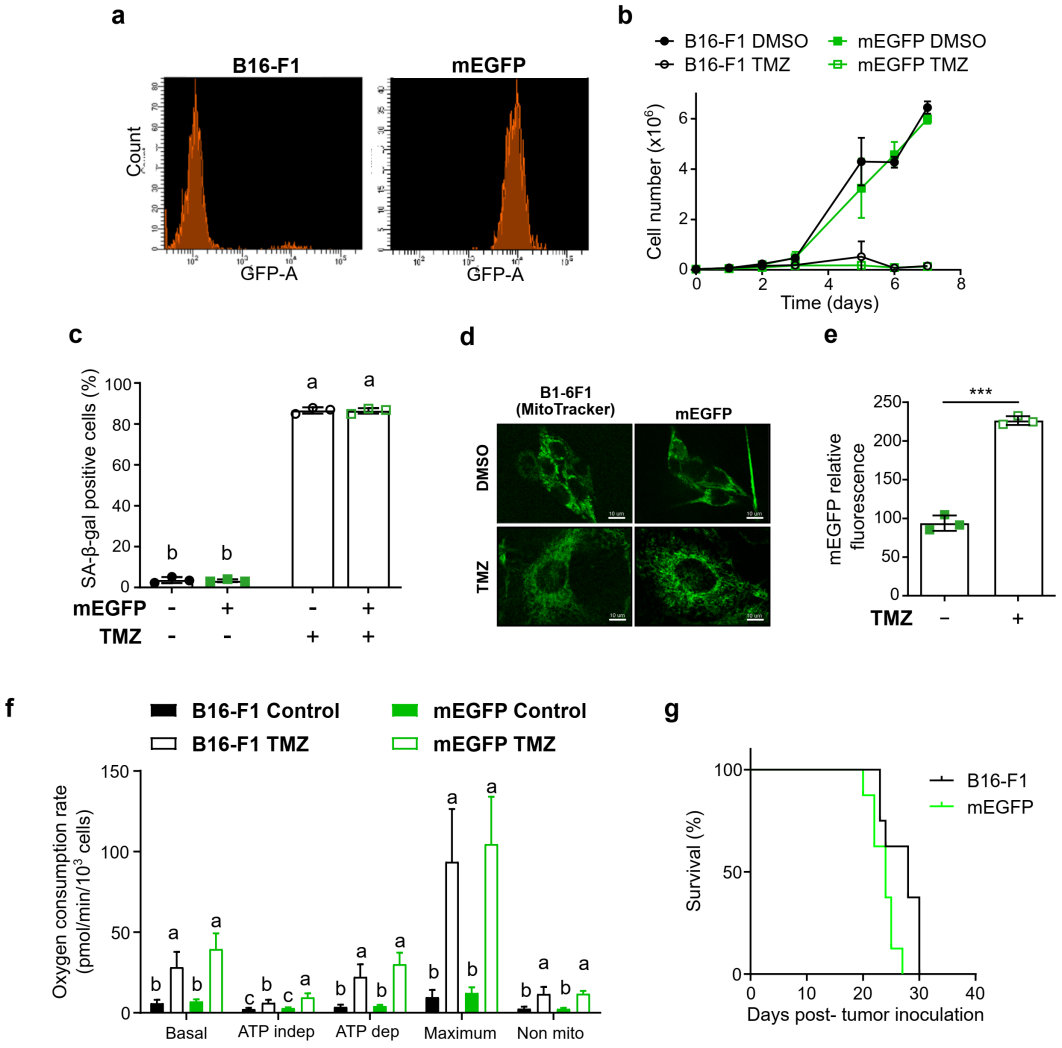


Figure S3: Generation of melanoma cells carrying a green fluorescent protein in the mitochondria. B16-F1 cells were transduced with lentiviral particles carrying the plasmid pLYS1-FLAG-MitoGFP-HA) and cells carrying the mEGFP protein were separated by cell sorting. B16-F1 and B16-F1-mEGFP cells were treated with DMSO or TMZ as described in Figure 1. **a** Histogram showing differences in fluorescence between B16-F1 and B16-F1-mEGFP cells after sorting. **b** Growth curve obtained by counting cell number (n=3). **c** Quantification of SA-β-gal activity (n = 3). **d** Confocal microscopy images of B16-F1 cells stained with MitoTracker Green FM and B16-F1 mEGFP cells. **e** Relative geometrical mean fluorescence intensity of B16-F1 mEGFP cells obtained by flow cytometry (n=3). **f** Respiratory parameters obtained from oxygen consumption rate (OCR) measurements before and following the sequential addition of oligomycin, FCCP and antimycin A (n = 5). **g** Kaplan-Meier survival curves for mice inoculated with B16-F1 or B16-F1-mEGFP cells. Results are the mean ± S.D. In **e** t-test was performed, *** $P < 0.0001$. In **b**, **c** and **f**, statistical significance was determined by two-way ANOVA, and Tukey post hoc for multiple comparisons. Groups with different letters are significantly different ($P < 0.05$).

Figure S4

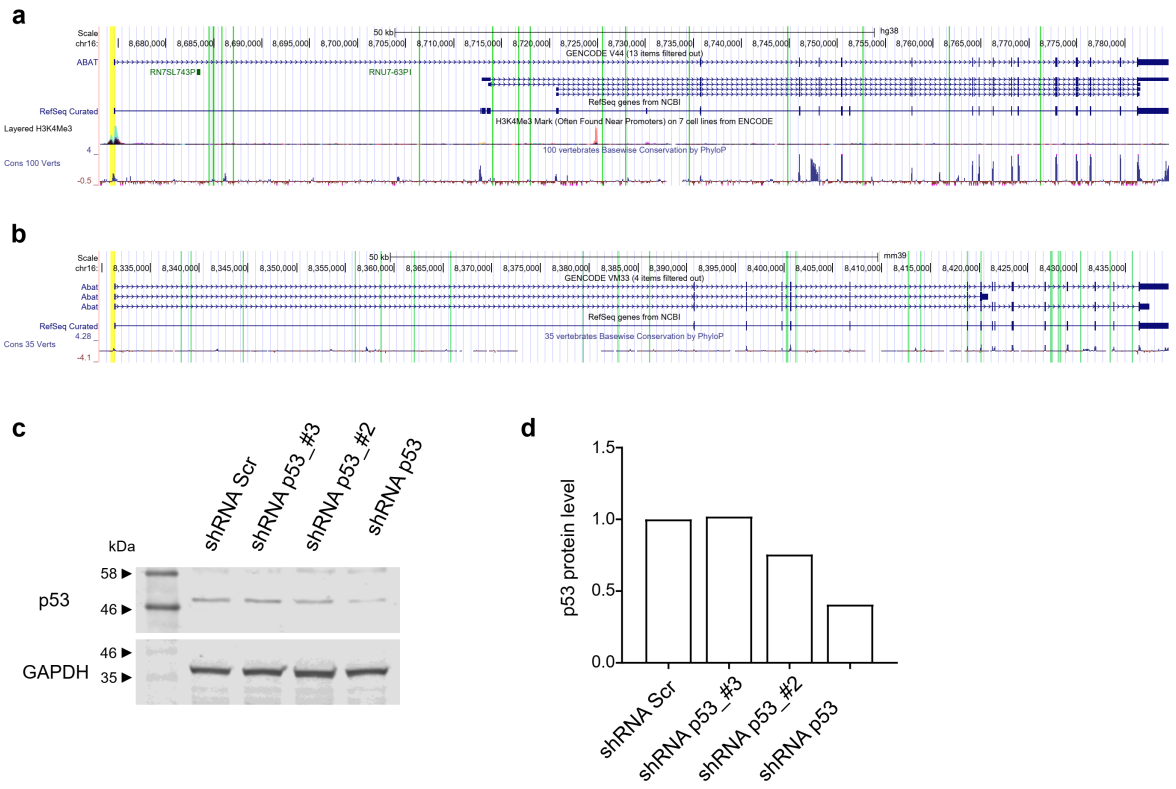


Figure S4: Genomic view of the human and mouse *Abat* gene in the UCSC browser and p53 silencing with different shRNAs. a and **b** Genomic view of the complete *Abat* gene plus 1.5 kb upstream of the gene start (promoter and proximal control gene region) in UCSC Genome Browser of human GRCh38/hg38 **(a)** and mouse GRCm39/mm39 **(b),** a 500bp bin highlighted in yellow in the promoter region. Bins highlighted in green are predicted binding sites for TP53 (JASPAR 2022 TFBS with score ≥400, which corresponds to p-value ≤ 10-4). Several gene annotation and ENCODE Project tracks for seven cell lines for human (GM12878, H1-hESC, HSMM, HUVEC, K562, NHEK, NHL) are displayed: histone modification (H3K4me3 marks the promoter region; color intensity is proportional to the maximum signal strength), conservation of the region of 100 vertebrates for human and 35 vertebrates for mouse (log-odds Phylop scores). The vertical viewing range of the tracks displays the default settings of the browser for each variable. **c** and **d** B16-F1 cells were transduced with lentiviral particles carrying short hairpin RNA (shRNA) with different sequences targeting *p53* or scrambled (Scr). **c** Western blots were performed with antibodies for p53 and GAPDH. **d** p53 levels were quantified from **(c)**, and normalized using GAPDH as a loading control.

Supplementary Table 3. Mitochondrial respiratory index. Coupling efficiency, Spare respiratory capacity, and respiratory control ratio were calculated from OCR measurements in Fig. 7g. Results are the mean ± S.D. Statistical significance of the main effects of TMZ treatment, PFT-α treatment and their interaction were determined by two-way ANOVA and Tukey post hoc for multiple comparisons. Groups with different letters are significantly different ($P < 0.05$). Main effects of TMZ treatment, PFT-α treatment, and their interaction, respectively, for: Coupling efficiency ($P < 0.0001$, $P < 0.05$, $P = 0.89$), Spare respiratory capacity ($P < 0.0001$, $P < 0.0001$, $P = 0.17$), Respiratory control ratio ($P < 0.0001$, $P < 0.01$, $P = 0.26$).

Respiratory ratios	Control - DMSO	Control - PFT-α	TMZ - DMSO	TMZ - PFT-α
Coupling efficiency	0.63 ± 0.02 [b]	0.57 ± 0.04 [b]	0.76 ± 0.02 [a]	0.70 ± 0.03 [a]
Spare respiratory capacity	1.8 ± 0.05 [d]	3.35 ± 0.11 [c]	3.92 ± 0.07 [b]	5.15 ± 0.38 [a]
Respiratory control ratio	4.98 ± 0.4 [c]	7.92 ± 0.7 [b]	16.2 ± 0.91 [a]	17.5 ± 2.5 [a]

Supplementary Table 4. Antibody list

Antibody	Dilution	Catalog number
Anti-P21	1:1000	#sc-6246 Santa Cruz Biotechnology
Anti-P53	1:1000	#sc-6243 Santa Cruz Biotechnology
Anti-ATM-P	1:1000	#05-740 Millipore
Anti-GAPDH	1:1000	#2118 Cell Signaling Technology
Anti-TUBULIN	1:1000	# Sigma-Aldrich
Anti-ABAT	1:10000	#ab108249 Abcam
Anti-SDH	1:1000	#ab14715 Abcam
Anti-puromycin	1:50	#MABE343-AF647

Supplementary Table 5. Primer list

Gene	Forward (5'-3')	Reverse (5'-3')
Mouse		
Abat	AGCTGAACACAATCCAGAATGC	ATACAGGTCCAACATGCGGTT
Cdkn1a (p21)	TCCAGACATTCAGAGCCACAGG	ACTTTGCTCCTGTGCGGAAC
Actb (β-Actin)	GCTTCTTTGCAGCTCCTTCGT	CGTCATCCATGGCGAACTG
Pgc1a (PGC1-α)	TGGAGTGACATAGAGTGTGCTGC	CTCAAATATGTTCGCAGGCTCA
Il6 (IL-6)	GTTCTCTGGGAAATCGTGGAAA	AAGTGCATCATCGTTGTTCATACA
Ccl2	ATTGGGATCATCTTGCTGGT	CCTGCTGTTCACAGTTGCC
Ccl5	CCACCTCCTCTCTGGGTTGG	GTGCCCACGTCAAGGAGTAT
mtDNA	ACCGCGGTCATACGATTAAC	CCCAGTTTGGGTCTTAGCTG
nDNA	AAAGCCACAAGAAACACTCAGGG	GACTCCCAGCACACTGAACTTAG
Human		
ABAT	CATGGGAGGACCATGGGTTG	GGGTATTTCAGCCGTGGGAA
ACTB (β-Actin)	CACCCAGCACAATGAAGATCA	CTCGTCATACTCCTGCTTGC

Uncropped Western blots

Fig. 2a

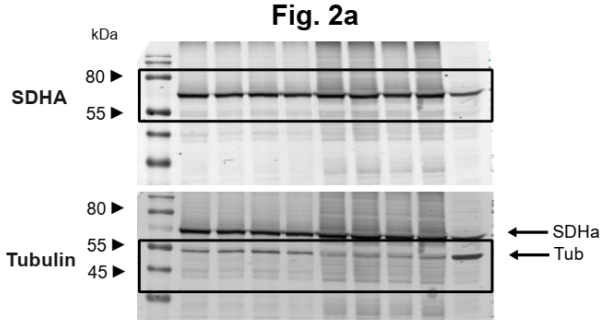


Fig. 4a

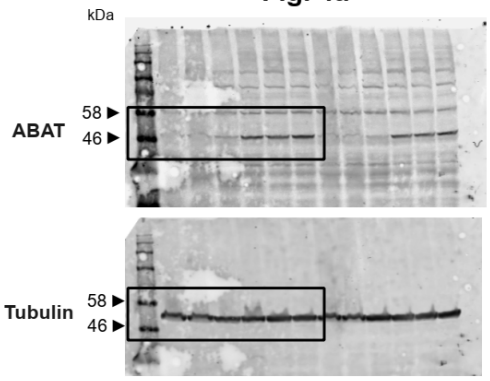


Fig. 7a

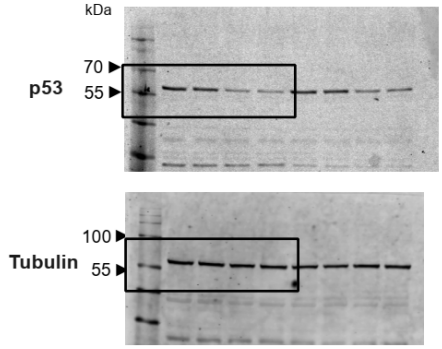


Fig. 8a

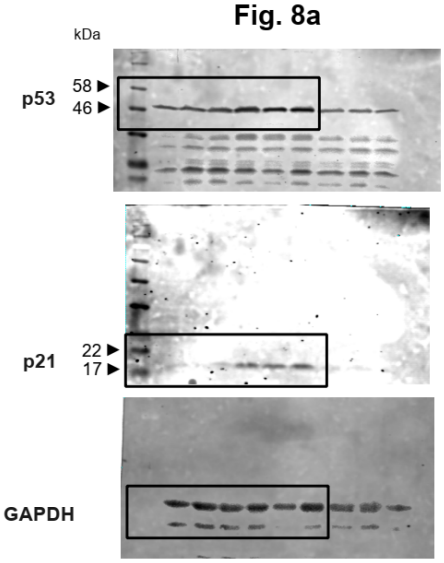


Fig. 8f

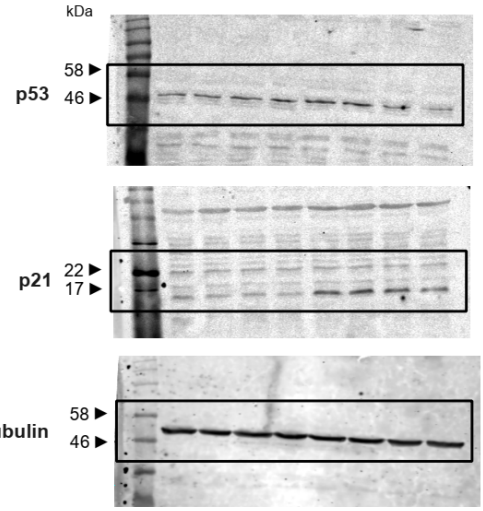


Fig. 8e

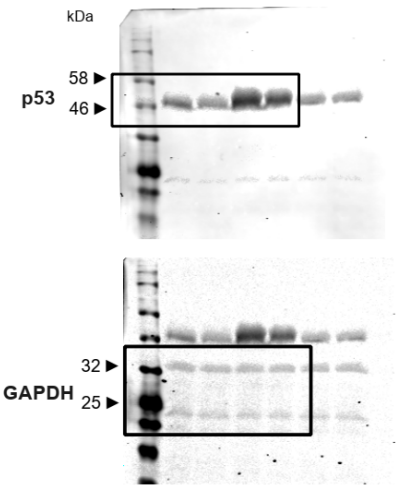


Fig. S4

